

High-order nonlinear Schrödinger equation and superluminal optical solitons in room-temperature active-Raman-gain media

Hui-jun Li,^{*} Chao Hang, and Guoxiang Huang[†]*State Key Laboratory Precision Spectroscopy, and Department of Physics, East China Normal University, Shanghai 200062, China*

L. Deng

Physics Laboratory, NIST, Gaithersburg, Maryland 20899, USA

(Received 10 May 2008; revised manuscript received 22 July 2008; published 13 August 2008)

We make a detailed study on the dynamics of gain-assisted superluminal optical solitons in a three-state active-Raman-gain medium at room temperature. Using a method of multiple-scales we derive a high-order nonlinear Schrödinger equation with correction terms contributed from differential gain, nonlinear dispersion, delay in nonlinear refractive index, and third-order dispersion of the system. We show that for a long pulse with realistic physical parameters the high-order correction terms are small and can be taken as perturbations. However, for a shorter pulse these higher-order correction terms are significant and hence must be treated on equal footing as the terms in the nonlinear Schrödinger equation. We provide exact soliton solutions of the higher-order nonlinear Schrödinger equation and demonstrate that such solitons have still superluminal propagating velocity and can be generated at very low light intensity.

DOI: [10.1103/PhysRevA.78.023822](https://doi.org/10.1103/PhysRevA.78.023822)

PACS number(s): 42.65.Tg, 05.45.Yv, 42.50.Md

I. INTRODUCTION

Optical solitons have been the subject of intensive theoretical and experimental studies for many years. These special types of optical wave packets appearing as the result of interplay between dispersion and nonlinearity are of special interest because of their important applications for information processing and transmission [1–4]. Up to now, most optical solitons are produced in passive optical media such as glass-based optical fibers, in which far-off resonance excitation schemes are generally employed in order to avoid unmanageable optical attenuation and distortion. As a result the nonlinear effect in such passive optical media is very weak, and hence to form a soliton a very high light intensity is required.

In recent years, much interest has focused on the wave propagation in highly resonant optical media via electromagnetically induced transparency (EIT) [5]. Due to the quantum interference effect induced by a control field, the wave propagation of a weak optical field in such medium displays many striking features [6], including a large suppression of optical absorption, a significant reduction of group velocity, and a giant enhancement of Kerr nonlinearity, etc. Based on these features, it has been shown that ultraslow optical solitons can form and propagate in various EIT media [7–10]. However, the weakly driven EIT-based scheme (i.e., the probe field is much smaller than the decay rate of the upper excited state and also much smaller than the control field) has drawbacks of large pulse spreading at room temperature and very long response time due to ultraslow propagation [11,12].

Since the work of Chiao and co-workers [13,14], the wave propagation in resonant optical media with an active-

Raman gain (ARG) have attracted considerable attention both theoretically and experimentally [15–30]. Contrary to the EIT-based scheme which is absorptive in nature, the central idea of the ARG scheme is that the signal field operates in the stimulated Raman emission mode, and hence the attenuation of the signal field can be completely eliminated and a stable superluminal propagation of the signal pulse can be realized [13–30]. In addition, it has been shown recently that a gain-assisted large and rapidly responding Kerr effect can also be obtained in a warm atomic vapor under the ARG scheme working at room temperature [11].

In a recent work, gain-assisted superluminal optical solitons in a three-level room-temperature ARG medium has been predicted [31]. A nonlinear Schrödinger (NLS) equation governing the motion of the envelope of signal optical field is derived. However, the calculation presented in Ref. [31] is based on the assumption of weak dispersion and weak nonlinearity and hence only low-order approximations of Maxwell-Schrödinger equations are taken into account. Obviously, for stronger dispersion and strong nonlinearity, or a larger propagating distance of the signal pulse, the results given in Ref. [31] are invalid and hence a new theoretical approach is needed.

In this work we present a detailed study of the propagation dynamics of a superluminal optical soliton in a three-state ARG system working at room temperature. By generalizing the method of multiple scales used in Ref. [31] we consider high-order approximations of Maxwell-Schrödinger equations and derive a high-order NLS equation for signal-field envelope. The high-order NLS equation includes the NLS equation obtained in Ref. [31] but with additional correction terms coming from differential gain, nonlinear dispersion, delay in nonlinear refractive index, and third-order dispersion of the system, which are absent in Ref. [31]. Furthermore, we show that for a realistic set of system parameters and for a long signal pulse these correction terms are indeed small and hence can be taken as perturbations. How-

^{*}Also at Department of Physics, Zhejiang Normal University, Jinhua 321004, Zhejiang, China.

[†]Corresponding author. gxhuang@phy.ecnu.edu.cn

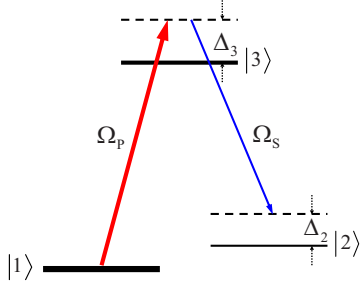


FIG. 1. (Color online) Excitation scheme of the three-state atomic system interacting with a strong, continuous-wave pump field with the one-half Rabi frequency Ω_P and a weak, pulsed signal field with the one-half Rabi frequency Ω_S . Δ_3 and Δ_2 are one-photon and two-photon detunings, respectively.

ever, for a shorter signal pulse these correction terms are significant and hence must be treated on the same footing as the terms in the NLS equation. We shall provide exact soliton solutions of the higher-order NLS equation, and demonstrate that such solitons have still a superluminal propagating velocity and can be produced at very low light intensity.

The paper is arranged as follows. In Sec. II, we give a simple introduction of the three-level ARG system under study. In Sec. III we derive the high-order NLS equation governing the motion of the envelope of the signal field. In Sec. IV, we present the gain-assisted superluminal optical soliton solutions for different pulse durations and discuss their stability. Finally, in Sec. IV we summarize the main results of our study.

II. MODEL

The model under consideration is a three-level atomic system working at room temperature, which interacts with a weak, pulsed signal field (with pulse length τ_0 at the entrance) and a strong, continuous-wave pump field (see Fig. 1). The pump field (with center angular frequency ω_P) and the signal field (with angular frequency ω_S) couple the transitions $|1\rangle \rightarrow |3\rangle$ and $|2\rangle \rightarrow |3\rangle$, respectively. The electric-field vector of the system reads $\mathbf{E} = \sum_{l=P,S} \mathbf{e}_l \mathcal{E}_l \exp[i(\mathbf{k}_l \cdot \mathbf{r} - \omega_l t)] + \text{c.c.}$, where $\mathbf{e}_l(\mathbf{k}_l)$ is the polarization direction (wave vector) of the electric field component with the envelope \mathcal{E}_l . The Hamiltonian of the system is given by $\hat{H} = \hat{H}_0 + \hat{H}'$, where \hat{H}_0 describes a free atom and \hat{H}' describes the interaction between the atom and the electric field, respectively. In the Schrödinger picture, the state vector of the system is $|\Psi(t)\rangle = \sum_{j=1}^3 a_j |j\rangle$, where $|j\rangle$ is the eigenvector of \hat{H}_0 and a_j is the probability amplitude of the state $|j\rangle$. Under electric-dipole and rotating-wave approximations, the Hamiltonian is given by

$$\hat{H} = \sum_{j=1}^3 \hbar \omega_j |j\rangle \langle j| - \hbar (\Omega_P e^{i(\mathbf{k}_P \cdot \mathbf{r} - \omega_P t)} |3\rangle \langle 1| + \Omega_S e^{i(\mathbf{k}_S \cdot \mathbf{r} - \omega_S t)} |3\rangle \langle 2| + \text{H.c.}), \quad (1)$$

where $\hbar \omega_j$ is the energy of the state $|j\rangle$, $\Omega_{P(S)} = (\mathbf{e}_{P(S)} \cdot \mathbf{p}_{31(32)}) \mathcal{E}_{P(S)} / \hbar$ is the one-half Rabi frequency of the

pump (signal) field, with \mathbf{p}_{ij} being the electric-dipole matrix element associated with the transition from $|j\rangle$ to $|i\rangle$, and H.c. represents Hermitian conjugate.

In order to investigate the time evolution of the system, it is more convenient to employ an interaction picture. We make the transformation $a_j = A_j \exp[i(\mathbf{k}_j \cdot \mathbf{r} - \omega_j t - \Delta_j t)]$, with $\mathbf{k}_1 = 0, \mathbf{k}_3 = \mathbf{k}_P, \mathbf{k}_2 = \mathbf{k}_P - \mathbf{k}_S$. Then, the Hamiltonian in the interaction picture reads as

$$\hat{H}_{\text{int}} = -\hbar \sum_{j=1}^3 \Delta_j |j\rangle \langle j| - \hbar (\Omega_P |3\rangle \langle 1| + \Omega_S |3\rangle \langle 2| + \text{H.c.}), \quad (2)$$

where $\Delta_3 = \omega_P - (\omega_3 - \omega_1)$ and $\Delta_2 = \omega_P - \omega_S - (\omega_2 - \omega_1)$ are the one- and two-photon detunings, respectively.

Using the Schrödinger equation $i\hbar \partial |\Psi(t)\rangle_{\text{int}} / \partial t = \hat{H}_{\text{int}} |\Psi(t)\rangle_{\text{int}}$, it is easy to obtain the equations for A_j ,

$$\left(i \frac{\partial}{\partial t} + d_2 \right) A_2 + \Omega_S^* A_3 = 0, \quad (3a)$$

$$\left(i \frac{\partial}{\partial t} + d_3 \right) A_3 + \Omega_P A_1 + \Omega_S A_2 = 0, \quad (3b)$$

with $|A_1|^2 + |A_2|^2 + |A_3|^2 = 1$. Here we have defined $d_{2,3} = \Delta_{2,3} + i\gamma_{2,3}$ with γ_j being the decay rates, introduced to represent the finite lifetime of the state $|j\rangle$.

The electric-field evolution is controlled by the Maxwell equation $\nabla^2 \mathbf{E} - (1/c^2) \partial^2 \mathbf{E} / \partial t^2 = (1/\epsilon_0 c^2) \partial^2 \mathbf{P} / \partial t^2$, where

$$\mathbf{P} = N(\mathbf{p}_{13} A_3 A_1^* \exp[i(\mathbf{k}_3 \cdot \mathbf{r} - \omega_P t)] + \mathbf{p}_{23} A_3 A_2^* \exp\{i[(\mathbf{k}_3 - \mathbf{k}_2) \cdot \mathbf{r} - \omega_S t]\} + \text{c.c.}).$$

Under a slowly varying envelope approximation, the Maxwell equation is reduced to

$$i \left(\frac{\partial}{\partial z} + \frac{1}{c} \frac{\partial}{\partial t} \right) \Omega_S + \kappa A_3 A_2^* = 0, \quad (4)$$

where $\kappa = N \omega_S |\mathbf{e}_S \cdot \mathbf{p}_{23}|^2 / (2\epsilon_0 \hbar c)$ with N being the atomic concentration. For simplicity, we have assumed $\mathbf{k}_S = \mathbf{e}_z k_S$.

We assume that atoms are initially populated in the state $|1\rangle$. Since the strong pump field couples the ground state, we require a large one-photon detuning. The role of this large one-photon detuning is twofold: (1) It keeps the gain at a manageable level and (2) it substantially reduces the complication due to Doppler broadening effect. The first feature provides an adjustable control of the gain whereas the second feature is important for room-temperature operation.

The lowest-order solution of Eqs. (3) is given by $A_1^{(0)} = 1/\sqrt{1+|\Omega_P/d_3|^2}$, $A_2^{(0)} = 0$, and $A_3^{(0)} = -\Omega_P/(d_3\sqrt{1+|\Omega_P/d_3|^2})$. The linear dispersion relation of the system is given by

$$K(\omega) = \frac{\omega}{c} + \frac{\kappa |A_3^{(0)}|^2}{\omega - d_2^*}. \quad (5)$$

$K(\omega)$ can be Taylor expanded around the center frequency of the probe field (corresponding to $\omega=0$), i.e., $K(\omega) = K_0 + K_1 \omega + \frac{1}{2} K_2 \omega^2 + \dots$, where the coefficients $K_j = [\partial^j K(\omega) / \partial \omega^j]_{\omega=0}$ ($j=0, 1, 2, \dots$) can be obtained from Eq.

(5) explicitly. Here $K_0 = \phi + i\alpha/2$ with $\phi = -\kappa|\Omega_P|^2\Delta_2/[|d_2|^2(|d_3|^2 + |\Omega_P|^2)]$ being a phase shift per unit length and $\alpha = -2\kappa|\Omega_P|^2\gamma_2/[|d_2|^2(|d_3|^2 + |\Omega_P|^2)]$ characterizes the absorption or gain of the signal field as it traverses the medium. Since $\alpha < 0$, we have a gain medium and the signal field grows as it propagates through the medium. It is precisely because of this signal field amplification during propagation that leads to the question of the possible Kerr self-induced nonlinearity and self-modulation effect. We also note that $\text{Re}[K_1]$ determines the group velocity and $\text{Im}[K_1]$ gives a further signal propagation gain. In addition, K_2 describes signal field group-velocity dispersion that contributes to both signal wave pulse spread and additional loss. In the remainder of this paper we investigate the possibility of actively balancing these signal pulse spreading and loss due to group-velocity dispersion by the signal gain due to K_0 and perhaps $\text{Im}[K_1]$.

III. ASYMPTOTIC EXPANSION AND A HIGH-ORDER NLS EQUATION

Now we apply a singular perturbation theory to solve Eqs. (3) and (4) in the nonlinear regime and search for the formation and propagation of a shape-preserving signal pulse in the system. We first note that nonvanishing two-photon detuning ($\Delta_2 \neq 0$) is necessary for producing a self-phase modulation effect that provides an effective mean to balance a detrimental dispersion effect, leading to the formation of a gain-assisted superluminal soliton. To get a quantitative description of the dynamics of such a soliton in the system, we first derive a nonlinear envelope equation that describes the evolution of the signal field envelope by employing the standard method of multiple scales [1]. Specifically, we make the following asymptotic expansion $A_j = \sum_{n=0}^{\infty} \epsilon^n A_j^{(n)}$ and $\Omega_S = \sum_{n=1}^{\infty} \epsilon^n \Omega_S^{(n)}$, where ϵ is a small parameter characterizing the amplitude of the signal field. To obtain a divergence-free expansion, all quantities on the right-hand side of the asymptotic expansion are considered as functions of the multiscale variables $z_l = \epsilon^l z$ ($l=0$ to 3) and $t_l = \epsilon^l t$ ($l=0, 1$). Substituting the expansion and the multiscale variables into Eqs. (3) and (4), we obtain the following linear inhomogeneous equations:

$$\left(i\frac{\partial}{\partial t_0} + d_2\right)A_2^{(j)} + \Omega_S^{*(j)}A_3^{(0)} = M^{(j)}, \quad (6a)$$

$$\left(i\frac{\partial}{\partial t_0} + d_3\right)A_3^{(j)} + \Omega_P A_1^{(j)} = N^{(j)}, \quad (6b)$$

$$i\left(\frac{\partial}{\partial z_0} + \frac{1}{c}\frac{\partial}{\partial t_0}\right)\Omega_S^{(j)} + \kappa A_3^{(0)}A_2^{*(j)} = Q^{(j)} \quad (j=1-4), \quad (6c)$$

where the explicit expressions of $M^{(j)}$, $N^{(j)}$, and $Q^{(j)}$ can be systematically and analytically obtained but they are omitted here.

For convenience, we convert Eqs. (6a)–(6c) into the following form:

$$\hat{L}\Omega_S^{(j)} = S^{(j)}, \quad (7a)$$

$$A_2^{(j)} = \frac{1}{\kappa A_3^{*(0)}} \left[Q^{*(j)} + i\left(\frac{\partial}{\partial z_0} + \frac{1}{c}\frac{\partial}{\partial t_0}\right)\Omega_S^{*(j)} \right], \quad (7b)$$

$$A_3^{(j)} = \frac{1}{d_3}(N^{(j)} - \Omega_P A_1^{(j)}), \quad (7c)$$

with

$$\hat{L} = i\left(\frac{\partial}{\partial z_0} + \frac{1}{c}\frac{\partial}{\partial t_0}\right)\left(-i\frac{\partial}{\partial t_0} + d_2^*\right) - \kappa|A_3^{(0)}|^2, \quad (8a)$$

$$S^{(j)} = \left(-i\frac{\partial}{\partial t_0} + d_2^*\right)Q^{(j)} - \kappa A_3^{(0)}M^{*(j)}, \quad (8b)$$

Equations (7a)–(7c) can be solved order by order in a simple and unified way.

(i) *First-order approximation.* The case for $j=1$ is just the linear problem solved in the last section. The linear dispersion relation is given by Eq. (5) and the first-order approximation solution reads as

$$\Omega_S^{(1)} = F e^{i\theta}, \quad (9a)$$

$$A_2^{(1)} = \frac{1}{\kappa A_3^{*(0)}} \left(K(\omega)^* - \frac{\omega}{c} \right) F^* e^{-i\theta^*}, \quad (9b)$$

$$A_3^{(1)} = A_1^{(1)} = 0, \quad (9c)$$

where $\theta = K(\omega)z_0 - \omega t_0$, F is a yet to be determined envelope function depending on the slow variables t_1 , z_1 , z_2 , and z_3 .

(ii) *Second-order approximation.* For $j=2$, we can obtain $S^{(2)}$ by using the first-order solution given by Eqs. (9a)–(9c) into M_2 and Q_2 . Then Eq. (7a) (for $j=2$) becomes

$$\hat{L}\Omega_S^{(2)} = i(\omega - d_2^*)\left(\frac{\partial}{\partial z_1} + \frac{1}{V_g}\frac{\partial}{\partial t_1}\right)F e^{i\theta}. \quad (10)$$

Notice that $\exp(i\theta)$ is an eigensolution of the operator \hat{L} ; divergence-free condition of the solution of Eq. (10) requires naturally

$$i\left(\frac{\partial F}{\partial z_1} + \frac{1}{V_g}\frac{\partial F}{\partial t_1}\right) = 0, \quad (11)$$

where $V_g = 1/K_1$ is (complex) group velocity of the wave packet. It is easy to find the second-order approximation solution as

$$\Omega_S^{(2)} = 0, \quad (12a)$$

$$A_1^{(2)} = b_1^{(2)}|F|^2 e^{-2\bar{\alpha}z_2}, \quad (12b)$$

$$A_3^{(2)} = b_3^{(2)}|F|^2 e^{-2\bar{\alpha}z_2}, \quad (12c)$$

$$A_2^{(2)} = \frac{i}{\kappa A_3^{*(0)}} \left(\frac{1}{c} - \frac{1}{V_g^*} \right) \frac{\partial F^*}{\partial t_1} e^{-i\theta^*}, \quad (12d)$$

where, $\bar{\alpha} = \epsilon^{-2}\alpha$. The explicit expressions of $b_1^{(2)}$ and $b_3^{(2)}$ have been listed in the Appendix.

(iii) *Third-order approximation.* Letting $j=3$ in Eq. (7) we obtain the third-order approximation equation for $\Omega_S^{(3)}$,

$$\hat{L}\Omega_S^{(3)} = (\omega - d_2^*) \left(i \frac{\partial}{\partial z_2} - \frac{1}{2} K_2 \frac{\partial^2}{\partial t_1^2} + W|F|^2 \right) F e^{i\theta}, \quad (13)$$

with

$$W = \frac{\kappa}{\omega - d_2^*} (A_3^{(0)} b_3^{*(2)} + A_3^{*(0)} b_3^{(2)}) e^{-2\bar{\alpha}z_2}.$$

Obviously, the divergence-free condition of Eq. (13) requires

$$i \frac{\partial F}{\partial z_2} - \frac{1}{2} K_2 \frac{\partial^2 F}{\partial t_1^2} + W|F|^2 F = 0. \quad (14)$$

Equation (14) is a NLS equation controlling the time evolution of the envelope function F , obtained in Ref. [31]. The coefficient W appearing in the third term of Eq. (14) characterizes the self-phase modulation of the signal field.

The third-order approximation solution is found to be

$$\Omega_S^{(3)} = 0, \quad (15a)$$

$$A_1^{(3)} = i \left(b_{11}^{(3)} \frac{\partial F}{\partial t_1} F^* + b_{12}^{(3)} \frac{\partial F^*}{\partial t_1} F \right) e^{-2\bar{\alpha}z_2}, \quad (15b)$$

$$A_3^{(3)} = i \left(b_{31}^{(3)} \frac{\partial F}{\partial t_1} F^* + b_{32}^{(3)} \frac{\partial F^*}{\partial t_1} F \right) e^{-2\bar{\alpha}z_2}, \quad (15c)$$

$$A_2^{(3)} = \left(-\frac{A_3^{(0)}}{(\omega - d_2)^3} \frac{\partial^2 F^*}{\partial t_1^2} + \frac{b_3^{(2)}}{\omega - d_2} |F|^2 F^* e^{-2\bar{\alpha}z_2} \right) e^{-i\theta^*}, \quad (15d)$$

where the coefficients $b_{11}^{(3)}$, $b_{12}^{(3)}$, $b_{31}^{(3)}$, and $b_{32}^{(3)}$ in the above expressions have been given in the Appendix.

(iv) *Fourth-order approximation.* To go beyond the work of Ref. [31], we should look for the high-order corrections further. Based on the solutions in the first-order to third-order approximations given above, from Eq. (7a) for $j=4$ we obtain

$$\hat{L}\Omega_S^{(4)} = i(\omega - d_2^*) \left(\frac{\partial F}{\partial z_3} - \frac{1}{6} K_3 \frac{\partial^3 F}{\partial t_1^3} + \beta_1 \frac{\partial(|F|^2 F)}{\partial t_1} + \beta_2 \frac{\partial(|F|^2)}{\partial t_1} F \right) e^{i\theta}, \quad (16)$$

where the coefficients β_1 and β_2 are given in the Appendix. The solvability condition of Eq. (16) gives rise to

$$\frac{\partial F}{\partial z_3} - \frac{1}{6} K_3 \frac{\partial^3 F}{\partial t_1^3} + \beta_1 \frac{\partial(|F|^2 F)}{\partial t_1} + \beta_2 \frac{\partial(|F|^2)}{\partial t_1} F = 0. \quad (17)$$

Combining Eqs. (11), (14), and (17), we obtain the following high-order NLS equation:

$$i \left(\frac{\partial}{\partial z} + \frac{1}{V_g} \frac{\partial}{\partial t} \right) U - \frac{1}{2} K_2 \frac{\partial^2 U}{\partial t^2} + W|U|^2 U + i \left(-\frac{K_3}{6} \frac{\partial^3 U}{\partial t^3} + \beta_1 \frac{\partial}{\partial t} (|U|^2 U) + \beta_2 \frac{\partial(|U|^2)}{\partial t} U \right) = 0, \quad (18)$$

where we have defined $U = \epsilon F$.

IV. DYNAMICS OF SUPERLUMINAL OPTICAL SOLITONS IN DIFFERENT PULSE DURATION REGIMES

Equation (18) derived in the preceding section is a high-order Ginzburg-Landau equation with complex coefficients and hence generally does not allow soliton solutions. However, if a realistic set of parameters can be found so that the imaginary part of these coefficients can be made small in comparison with their corresponding real parts, then it is possible to get a shape-preserving, localized signal pulse that can propagate for an extended distance without significant attenuation and distortion. We shall show this is indeed possible for the present gain-assisted system. A set of realistic parameters of the system will be given below.

With a small imaginary part of the coefficients, Eq. (18) can be converted into the dimensionless high-order NLS equation

$$i \frac{\partial u}{\partial s} + \frac{\partial^2 u}{\partial \sigma^2} + 2|u|^2 u = i \left(g_0 u + g_1 \frac{\partial(|u|^2 u)}{\partial \sigma} + g_2 u \frac{\partial(|u|^2)}{\partial \sigma} + g_3 \frac{\partial^3 u}{\partial \sigma^3} \right) + g_4 \frac{\partial u}{\partial \sigma}, \quad (19)$$

where we have taken $\omega=0$ (corresponding to the central frequency of the signal field) and defined $U = U_0 \mu e^{\alpha z}$, $s = z/(2L_D)$, and $\sigma = [t - z/\text{Re}(V_g)]/\tau_0$. The coefficients $g_j = 2L_D/L_j$ ($j=0$ to 4), where $L_0 = -1/\alpha$ (characteristic linear gain length), $L_1 = -\tau_0/(\beta_{1r} U_0^2)$ (characteristic nonlinear dispersion length), $L_2 = -\tau_0/(\beta_{2r} U_0^2)$ (characteristic delay length in nonlinear refractive index), $L_3 = 6\tau_0^3/K_{3r}$ (characteristic third-order dispersion length), and $L_4 = \tau_0/K_{1i}$ (characteristic differential gain length), respectively. Here, subscripts r and i denote, respectively, the real and imaginary parts of corresponding quantities. $L_D = -\tau_0^2/K_{2r}$ is the characteristic dispersion length at which the group velocity dispersion becomes important. Obviously, the property of the formation and propagation of solitons in the system is controlled by these characteristic lengths. For the balance between the dispersion and nonlinearity, we have taken $L_D = L_{NL}$, where $L_{NL} = 1/(W_r U_0^2)$ is the characteristic nonlinear length. Thus, we obtain $U_0 = \sqrt{|K_{2r}/W_r|}/\tau_0$, which is a typical one-half Rabi frequency of the probe field. In the following, we discuss two cases of soliton excitations in the system based on the high-order NLS equation (19).

Case 1: Soliton solutions for perturbed NLS equation. If L_j ($j=0$ to 4) are much larger than L_D , the terms on the right-hand side of Eq. (19) are high-order small corrections to the NLS equation and hence can be taken as perturbations,

which are not considered in the simple approach given in Ref. [31]. We now consider the effect of these perturbations to a soliton. We write Eq. (19) in the following form:

$$i\frac{\partial u}{\partial s} + \frac{\partial^2 u}{\partial \sigma^2} + 2|u|^2 u = iR[u], \quad (20)$$

where $R[u] = g_0 u + g_1 \partial(|u|^2 u) / \partial \sigma + g_2 u \partial(|u|^2) / \partial \sigma + g_3 \partial^3 u / \partial \sigma^3 - i g_4 \partial u / \partial \sigma$, representing the perturbations. We use the standard soliton perturbation theory [33] to solve the perturbed NLS equation (20). The soliton solution of Eq. (20) for $R[u]=0$ reads as

$$u_0 = 2\rho \operatorname{sech}[2\rho(\sigma - \sigma_0 + 4\mu s)] \times \exp[-2i\mu\sigma - 4i(\mu^2 - \rho^2)s - i\psi_0], \quad (21)$$

where $\mu, \rho, \sigma_0, \psi_0$ are real, free parameters determining the initial propagating velocity, amplitude (as well as width), position, and phase of the soliton, respectively. When the perturbations take action, i.e., $R[u] \neq 0$, these soliton parameters will change and depend on the propagation distance z . Solving the ordinary differential equations of $\mu(z), \rho(z), \sigma_0(z)$, and $\psi_0(z)$ based on the soliton perturbation theory [33] we obtain the adiabatic evolution of the soliton (21), which is given by

$$\Omega_s = \frac{e^{g_0 z / L_D}}{\tau_0} \sqrt{-K_{2r} / W_r} \operatorname{sech} \left[\frac{e^{g_0 z / L_D}}{\tau_0} \left(t - \frac{z}{V_{gr}} + 2 \frac{\mu \tau_0}{L_D} z \right) \right] \exp \left[i K_{0r} z - 2i\mu \left(t - \frac{z}{V_{gr}} \right) / \tau_0 - 4i \frac{(\mu^2 - \rho^2)}{2L_D} z \right], \quad (22)$$

where $\mu = -g_4 [\exp(2g_0 z / L_D) - 1] / (12g_0)$, $\rho = (1/2) \exp(g_0 z / L_D)$. We see that the perturbations result in not only an increasing in the soliton amplitude and decreasing in the soliton width, but also a change of the propagating velocity and a shift of oscillating frequency [34].

Case 2. Soliton solutions for the high-order NLS equation. If some of L_j ($j=0-4$) are of the same magnitude of order as L_D , the terms on the right-hand side of Eq. (19) become significant and cannot be taken as perturbations. In this situation, Eq. (19) reduces to the high-order NLS equation

$$i\frac{\partial u}{\partial s} + \frac{\partial^2 u}{\partial \sigma^2} + 2|u|^2 u - i \left(g_1 \frac{\partial(|u|^2 u)}{\partial \sigma} + g_2 u \frac{\partial|u|^2}{\partial \sigma} + g_3 \frac{\partial^3 u}{\partial \sigma^3} \right) = 0, \quad (23)$$

if the condition $g_0, g_4 \ll g_1, g_2, g_3$ can be satisfied. Equation (23) supports the exact soliton solution [32]

$$\Omega_s = U_0 \left(\frac{3(\beta + 3q^2 - 2q)}{g_3^2(3c_1 + 2c_2)} \right)^{1/2} \times \operatorname{sech} \left[\frac{\sqrt{\beta + 3q^2 - 2q}}{g_3} \left(\frac{t - z/V_{gr}}{\tau_0} + \frac{\beta z}{2g_3 L_D} \right) \right] \times \exp \left(i[q^3 - q^2 + (\beta + 3q^2 - 2q)(1 - 3q)] \right) \times \frac{z}{2g_3^2 L_D} - i \frac{q}{g_3} \frac{t - z/V_{gr}}{\tau_0} + i\phi z, \quad (24)$$

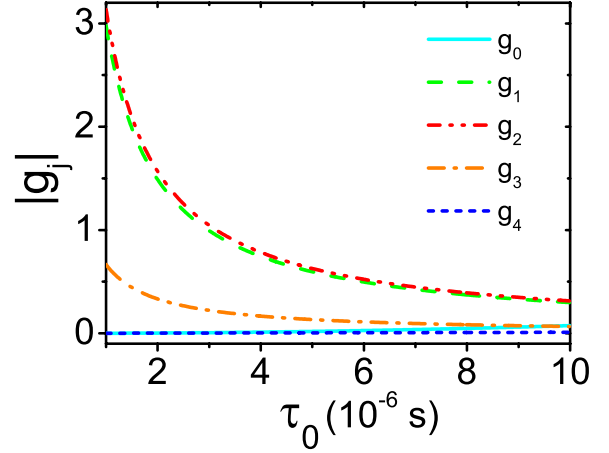


FIG. 2. (Color online) The absolute value of the coefficients g_j ($j=0-4$) of Eq. (19) as functions of the pulse length τ_0 . Parameters are given in the text.

with the conditions $\beta + 3q^2 - 2q > 0$, $3q_1 + 2q_2 > 0$, and $q \neq 1/3$, where β is a free real number, $c_1 = g_1 / (2g_3)$, $c_2 = g_2 / (2g_3)$, and $q = (3c_1 + 2c_2 - 3) / [6(c_1 + c_2)]$.

To demonstrate that the imaginary parts of the coefficients of Eq. (18) can be much less than their corresponding real parts, we consider a set of parameters relevant to a typical alkali atom vapor working at room temperature. For such system (e.g., ^{87}Rb warm vapor at temperature 300 K), Doppler effect may contribute linewidth broadening around 500 MHz, which may degrade the effectiveness of the EIT-based scheme. It is, however, much less important in an ARG-based scheme because we can choose a large one-photon detuning Δ_3 [11] to suppress the Doppler effect. This aim can be easily reached by taking $\Delta_3 = -2.0$ GHz in the present system. The other parameters are given by $\gamma_2 \approx 500$ Hz, $\gamma_3 \approx 500$ MHz (such big γ_3 is mainly due to Doppler broadening), $\kappa\tau_0 = 8000.0 \text{ cm}^{-1}$, $\Delta_2\tau_0 = 1.5$, $\Delta_3\tau_0 = -2000$, and $\Omega_p\tau_0 = 43.0$ with $\tau_0 = 1.0 \mu\text{s}$. With the above parameters, we obtain $K_0 = -(2.32 + i0.77 \times 10^{-3}) \text{ cm}^{-1}$, $K_1 = -(15.46 + i0.01) \times 10^{-7} \text{ cm}^{-1} \text{ s}$, $K_2 = -(20.62 + i0.02) \times 10^{-13} \text{ cm}^{-1} \text{ s}^2$, $K_3 = -(41.23 + i0.05) \times 10^{-19} \text{ cm}^{-1} \text{ s}^3$, $W = (19.03 + i0.006) \times 10^{-16} \text{ cm}^{-1} \text{ s}^2$, $\beta_1 = (28.4 + i0.01) \times 10^{-22} \text{ cm}^{-1} \text{ s}^3$, and $\beta_2 = -(2.99 + i0.24) \times 10^{-21} \text{ cm}^{-1} \text{ s}^3$. We see that the imaginary part of every coefficient of the high-order Ginzburg-Landau equation (18) is indeed much smaller than its real part, justifying the validity of the high-order NLS equation (19). With these results we obtain the group velocity of the soliton (24) as

$$\operatorname{Re}(V_g) = -0.58 \times 10^{-5} c. \quad (25)$$

Hence, the soliton obtained travels with a superluminal propagating velocity.

In order to show in what physical condition the solitons given by (22) and (24) can form in the system, in Fig. 2 we have plotted the curves of the absolute value of the coefficients g_j ($j=1-4$) as functions of the pulse length τ_0 . (The other parameters are the same as given above.) We see that g_0 and g_4 are not sensitive to τ_0 , but g_1, g_2 , and g_3 decrease rapidly when τ_0 increases. Thus, in different pulse duration

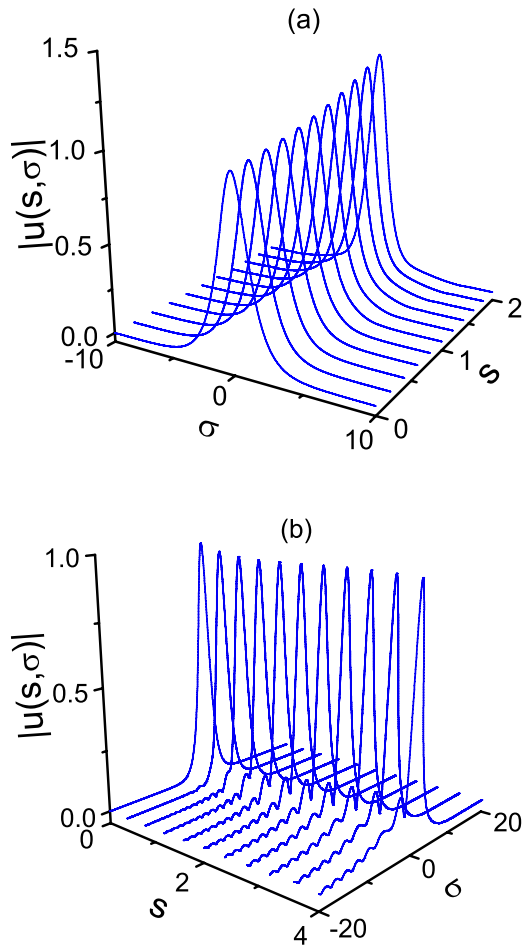


FIG. 3. (Color online) Evolution of superluminal optical soliton based on the perturbed NLS equation (20). $|u(s, \sigma)|$: Dimensionless amplitude. s : Dimensionless propagating distance. σ : Dimensionless delay time. The input condition is taken as $u(0, \sigma) = \text{sech } \sigma$. (a) $\tau_0 = 1.0 \times 10^{-5}$ s. (b) $\tau_0 = 1.0 \times 10^{-6}$ s. Other parameters are the same as those in Fig. 2.

regions, we can reduce Eq. (19) into different models. From the figure we obtain the following conclusions: (1) If $\tau_0 \geq 8.0 \times 10^{-6}$ s, all g_j are small and hence the terms on the right-hand side of Eq. (19) can be taken as high-order correction terms. In this case Eq. (19) can be taken as a NLS equation plus perturbations, so the perturbed soliton solution (22) is valid. (2) When $\tau_0 \leq 4.0 \times 10^{-6}$ s, g_1, g_2 , and g_3 become order unity and the condition $g_0, g_4 \ll g_1, g_2, g_3$ is satisfied. Consequently, Eq. (19) in this case can be reduced to Eq. (23) and so the system allows the soliton solution given by (24).

It is instructive to discuss and compare the physical properties of the solitons given by Eqs. (22) and (24). We study this problem by using numerical simulations. The results are presented in Figs. 3 and 4. From Fig. 2 we see that to make the perturbed NLS equation (20) be valid the pulse length τ_0 should be around 10^{-5} s. Shown in Fig. 3(a) is the time evolution of the soliton obeying the perturbed NLS equation (20) by taking $u(0, \sigma) = \text{sech } \sigma$ as input condition. The pulse length is chosen as $\tau_0 = 1.0 \times 10^{-5}$ s and the other parameters are the same as those in Fig. 2. We see that in this case the

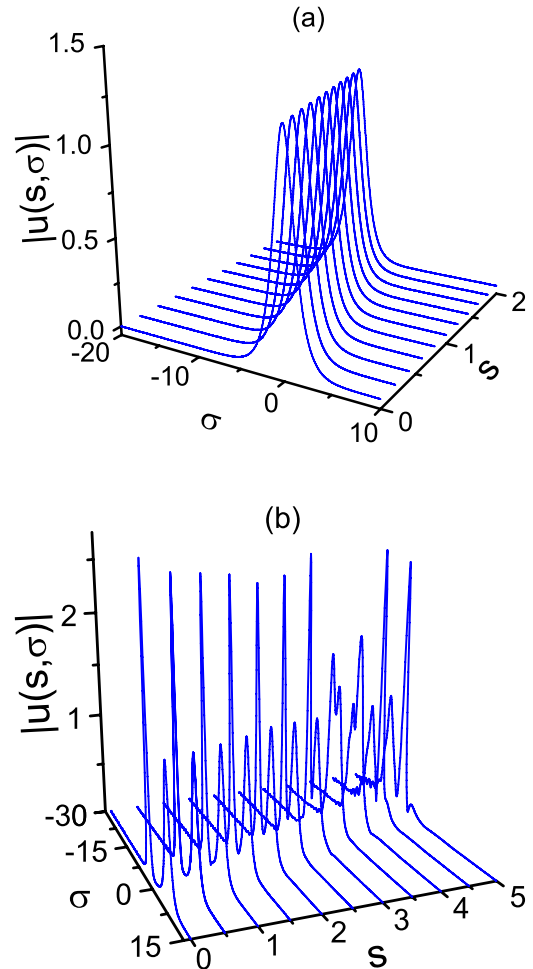


FIG. 4. (Color online) Evolution and collision of superluminal optical soliton based on the high-order NLS equation (23) with pulse length $\tau_0 = 1.0 \times 10^{-6}$ s and other parameters the same as Fig. 2. $|u(s, \sigma)|$: Dimensionless amplitude. s : Dimensionless propagating distance. σ : Dimensionless delay time. (a): Soliton evolution with input condition $u(0, \sigma) = 1.23 \text{ sech } \sigma \exp(i2.12\sigma)$. (b) Two-soliton collision with input condition $u(0, \sigma) = 1.23 \text{ sech}(\sigma - 5.0) \exp[i2.12(\sigma - 5.0)] + 2.71 \text{ sech}[2.21(\sigma + 5.0)] \exp[i2.12(\sigma + 5.0)]$.

soliton is fairly stable during propagation. However, there is a small increase of the soliton amplitude when propagating to large distance, contributed from the perturbed term $R[u]$ on the right-hand side of Eq. (20). $R[u]$ is in fact a gain due to the gain character of the system.

Figure 3(b) shows the simulation result based on the perturbed NLS equation (20) but taking the pulse length $\tau_0 = 1.0 \times 10^{-6}$ s. One can see that the soliton radiates many ripples even propagating to only a small distance. The reason for such instability is that in this case the perturbed NLS equation (20) is no longer valid. This point can be clearly seen in Fig. 2, which shows that for the pulse length τ_0 around 10^{-6} s, the coefficients g_j ($j=1, 2, 3$) become larger and hence break down the validity condition of Eq. (20).

To check the stability of the soliton solution of the high-order NLS equation, we have made additional numerical simulation based on Eq. (23). Shown in Fig. 4(a) is the simu-

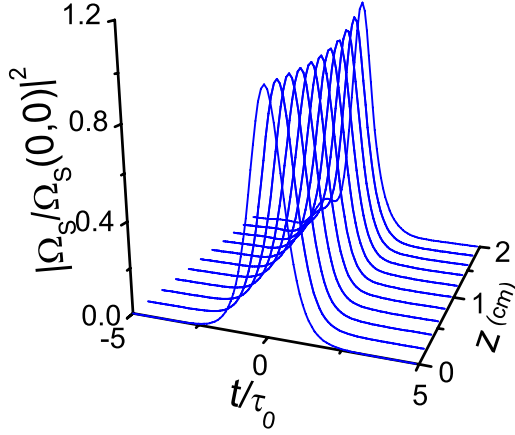


FIG. 5. (Color online) The result of numerical simulation starting directly from Eqs. (3) and (4) by taking the soliton solution (24) of the high-order NLS equation as input condition. The parameters given are the same as in Fig. 2 (with $\tau_0 = 1.0 \times 10^{-6}$ s), the input pulse is $\Omega_s(0, t)\tau_0 = 40.6 \operatorname{sech}(t/\tau_0) \exp(i2.1t/\tau_0)$.

lation result for the single soliton solution of Eq. (23) by choosing $u(0, \sigma) = 1.23 \operatorname{sech} \sigma \exp(i2.12\sigma)$ as input condition. We choose $\beta = -2.73$ and the other parameters are the same as those in Fig. 2. We see that the soliton is fairly stable after propagating a long distance. The reason is that in this case there is exact balance between high-order dispersion and high-order nonlinearity in Eq. (23).

We have also investigated the two-soliton collision of the high-order NLS equation (23). The result is demonstrated in Fig. 4(b). The input condition is taken as $u(0, \sigma) = 1.23 \operatorname{sech}(\sigma - 5.0) \exp[i2.12(\sigma - 5.0)] + 2.71 \operatorname{sech}[2.21(\sigma + 5.0)] \exp[i2.12(\sigma + 5.0)]$. One can see that the solitons preserve their wave shapes after the collision.

We have made also a numerical simulation based directly on the Maxwell-Schrödinger equations (3) and (4) to check the validity of the approximations used in our analytical approach given in Secs. II and III. Shown in Fig. 5 is the soliton evolution when taking the soliton solution (24) as an input condition. From the figure we see that the soliton solution of the high-order NLS equation is fairly stable for a very long propagating distance. Different from the EIT-based systems [7–10], where solitons always have a small decay in amplitude due to inherent absorption, the soliton in the present gain-assistant system has a growth in amplitude. However, the increase in amplitude can be suppressed by using a large one-photon detuning $|\Delta_3|$.

We now estimate the light intensity for generating the optical soliton (24). It is easy to show that the peak power of the gain-assisted superluminal optical soliton, i.e., Eq. (24), is given by $\bar{P}_{\max} = 2\epsilon_0 c n_S S_0 (\hbar/|\mathbf{p}_{23}|)^2 U_0^2 [3(\beta + 3q^2 - 2q)] / [g_3^2(3c_1 + 2c_2)]$. Here n_S is the reflective index of the signal field and S_0 is the cross-section area of the signal field. Taking $S_0 = 1.0 \times 10^{-4}$ cm², $|\mathbf{p}_{23}| = 2.1 \times 10^{-27}$ cm C, and using the parameters given above, we obtain $\bar{P}_{\max} = 2.2$ μ W. Consequently, to generate the gain-assisted superluminal optical soliton based on the high-order NLS equation (18), very low input light intensity is needed. This is drastically different from the optical soliton generation schemes in fiber-

based passive media, where much higher input power is required in order to bring out the nonlinear effect required for the soliton formation.

V. SUMMARY

We have presented a detailed investigation on the dynamics of a superluminal optical soliton in a gain-assisted three-state system working at room temperature. By using a method of multiple scales we have derived a higher-order NLS equation, which includes effects of linear and differential gain, nonlinear dispersion, delay in nonlinear refractive index, and third-order dispersion. We have shown that for a realistic set of physical parameters and for a long pulse duration the high-order correction terms obtained are small enough and hence can be taken as perturbations. However, for a short pulse duration these correction terms are significant and cannot be considered as perturbations, i.e., they must be treated on the same footing as the terms in the NLS equation. We have provided exact soliton solutions for the high-order NLS equation, which propagate with a superluminal propagating velocity and can be generated with very low input light intensity. The stability of the gain-assisted superluminal optical solitons obtained has been checked by numerical simulations. Due to their robust propagating nature and very low generation power, the gain-assisted superluminal optical solitons predicted here may have potential applications in optical information processing and engineering.

ACKNOWLEDGMENTS

This work was supported by the National Natural Science Foundation of China under Grants No. 10434060 and No. 10674060, by the Key Development Program for Basic Research of China under Grants No. 2005CB724508 and No. 2006CB921104, and by the Program for Changjiang Scholars and Innovative Research Team of the Chinese Ministry of Education.

APPENDIX: COEFFICIENTS IN SEC. III

The coefficients $b_1^{(2)}$ and $b_3^{(2)}$ in Eqs. (12) are given by

$$b_1^{(2)} = \frac{|A_3^{(0)}|^2}{2A_1^{(0)}(|d_3|^2 + |\Omega_P|^2)} \frac{(\omega - d_2^*)d_3^* + (\omega - d_2)d_3 - |d_3|^2}{|\omega - d_2|^2}, \quad (\text{A1a})$$

$$b_3^{(2)} = -\frac{A_3^{(0)}}{d_3(\omega - d_2)} - \frac{\Omega_P}{d_3} b_1^{(2)}. \quad (\text{A1b})$$

The coefficients $b_{11}^{(3)}$, $b_{12}^{(3)}$, $b_{31}^{(3)}$, and $b_{32}^{(3)}$ in Eqs. (15) are

$$b_{11}^{(3)} = -\frac{|d_3|^2}{2A_1^{(0)}(|d_3|^2 + |\Omega_P|^2)} \left(-\frac{|A_3^{(0)}|^2}{|\omega - d_2|^2(\omega - d_2^*)} + \frac{|A_3^{(0)}|^2}{d_3^*(\omega - d_2^*)^2} + \frac{A_3^{(0)} b_3^{*(2)}}{d_3^*} - \frac{A_3^{*(0)} b_3^{(2)}}{d_3} \right), \quad (\text{A2a})$$

$$b_{12}^{(3)} = -\frac{|d_3|^2}{2A_1^{(0)}(|d_3|^2 + |\Omega_P|^2)} \left(\frac{|A_3^{(0)}|^2}{|\omega - d_2|^2(\omega - d_2)} - \frac{|A_3^{(0)}|^2}{d_3(\omega - d_2)^2} + \frac{A_3^{(0)}b_3^{*(2)}}{d_3^*} - \frac{A_3^{*(0)}b_3^{(2)}}{d_3} \right), \quad (\text{A2b})$$

$$b_{31}^{(3)} = -\frac{1}{d_3}(b_3^{(2)} + \Omega_P b_{11}^{(3)}), \quad (\text{A2c})$$

$$b_{32}^{(3)} = -\frac{1}{d_3} \left(b_3^{(2)} + \frac{A_3^{(0)}}{(\omega - d_2)^2} + \Omega_P b_{12}^{(3)} \right). \quad (\text{A2d})$$

The coefficients β_1 and β_2 in Eq. (16) are given by

$$\beta_1 = \kappa |A_3^{(0)}|^2 \frac{e^{-2\bar{\alpha}z_2}}{\omega - d_2^*} \left(\frac{1}{|\omega - d_2|^2 d_3} + \frac{2}{(\omega - d_2^*)^2 d_3^*} + \frac{1}{(\omega - d_2)^2 d_3} + \frac{\delta}{\omega - d_2^*} - \frac{|\Omega_P|^2(G^* + G)}{|d_3|^2 + |\Omega_P|^2} \right), \quad (\text{A3a})$$

$$\beta_2 = \kappa |A_3^{(0)}|^2 \frac{e^{-2\bar{\alpha}z_2}}{\omega - d_2^*} \left(\frac{|\Omega_P|^2(G^* + 2G)}{|d_3|^2 + |\Omega_P|^2} - \frac{\delta}{2(\omega - d_2^*)} - \frac{1}{|\omega - d_2|^2 d_3} + \frac{\delta}{2d_3} - \frac{\delta}{2d_3^*} + \frac{1}{(\omega - d_2)d_3^2} - \frac{1}{(\omega - d_2^*)d_3^{*2}} - \frac{2}{(\omega - d_2)^2 d_3} - \frac{1}{(\omega - d_2^*)^2 d_3^*} \right), \quad (\text{A3b})$$

with

$$\delta = \frac{|\Omega_P|^2[|d_3|^2 - (\omega - d_2)d_3 - (\omega - d_2^*)d_3^*]}{|\omega - d_2|^2 |d_3|^2 (|\Omega_P|^2 + |d_3|^2)},$$

$$G = -\frac{1}{|\omega - d_2|^2(\omega - d_2)} + \frac{1}{(\omega - d_2)^2 d_3} - \frac{1}{(\omega - d_2)d_3^2} + \frac{1}{(\omega - d_2^*)d_3^{*2}} + \frac{\delta(d_3 - d_3^*)}{2|d_3|^2}.$$

-
- [1] A. Hasegawa and M. Matsumoto, *Optical Solitons in Fibers* (Springer, Berlin, 2003).
- [2] G. P. Agrawal, *Nonlinear Fiber Optics* (Academic, New York, 2001).
- [3] Y. S. Kivshar and G. P. Agrawal, *Optical Solitons: From Fibers to Photonic Crystals* (Academic, San Diego, 2003).
- [4] B. A. Malomed, *Soliton Management in Periodic Systems* (Springer, New York, 2006).
- [5] S. E. Harris, *Phys. Today* **50**(7), 36 (1997).
- [6] M. Fleischhauer, A. Imamoglu, and J. P. Marangos, *Rev. Mod. Phys.* **77**, 633 (2005), and references therein.
- [7] Y. Wu and L. Deng, *Phys. Rev. Lett.* **93**, 143904 (2004).
- [8] G. Huang, L. Deng, and M. G. Payne, *Phys. Rev. E* **72**, 016617 (2005); G. Huang, K. Jiang, M. G. Payne, and L. Deng, *ibid.* **73**, 056606 (2006).
- [9] L. Deng, M. G. Payne, G. Huang, and E. W. Hagley, *Phys. Rev. E* **72**, 055601(R) (2005).
- [10] C. Hang and G. Huang, *Phys. Rev. A* **77**, 033830 (2008).
- [11] L. Deng and M. G. Payne, *Phys. Rev. Lett.* **98**, 253902 (2007).
- [12] K. J. Jiang, L. Deng, E. W. Hagley, and M. G. Payne, *Phys. Rev. A* **77**, 045804 (2008).
- [13] R. Y. Chiao, *Phys. Rev. A* **48**, R34 (1993).
- [14] A. M. Steinberg and R. Y. Chiao, *Phys. Rev. A* **49**, 2071 (1994); R. Y. Chiao and A. M. Steinberg, in *Progress in Optics*, edited by E. Wolf (Elsevier, Amsterdam, 1997), p. 345.
- [15] L. J. Wang, A. Kuzmich, and A. Dogariu, *Nature (London)* **406**, 277 (2000).
- [16] A. Dogariu, A. Kuzmich, and L. J. Wang, *Phys. Rev. A* **63**, 053806 (2001).
- [17] A. Kuzmich, A. Dogariu, L. J. Wang, P. W. Milonni, and R. Y. Chiao, *Phys. Rev. Lett.* **86**, 3925 (2001).
- [18] A. M. Akulshin, A. Cimmino, and D. I. Opat, *Quantum Electron.* **32**, 567 (2002).
- [19] A. M. Akulshin, A. Cimmino, A. I. Sidorov, P. Hannaford, and G. I. Opat, *Phys. Rev. A* **67**, 011801(R) (2003).
- [20] A. Lezama, A. M. Akulshin, A. I. Sidorov, and P. Hannaford, *Phys. Rev. A* **73**, 033806 (2006).
- [21] M. S. Bigelow, N. N. Lepeshkin, and R. W. Boyd, *Science* **301**, 200 (2003).
- [22] M. D. Stenner, D. J. Gauthier, and M. A. Neifield, *Nature (London)* **425**, 695 (2003).
- [23] M. D. Stenner and D. J. Gauthier, *Phys. Rev. A* **67**, 063801 (2003).
- [24] R. G. Ghulghazaryan and Y. P. Malakyan, *Phys. Rev. A* **67**, 063806 (2003).
- [25] K. Kim, H. S. Moon, C. Lee, S. K. Kim, and J. B. Kim, *Phys. Rev. A* **68**, 013810 (2003).
- [26] L.-G. Wang, N.-H. Liu, Q. Lin, and S.-Y. Zhu, *Phys. Rev. E* **68**, 066606 (2003).
- [27] E. E. Mikhailov, V. A. Sautenkov, I. Novikova, and G. R. Welch, *Phys. Rev. A* **69**, 063808 (2004).
- [28] M. Janowicz and J. Mostowski, *Phys. Rev. E* **73**, 046613 (2006).
- [29] K. J. Jiang, L. Deng, and M. G. Payne, *Phys. Rev. A* **74**, 041803(R) (2006).
- [30] J. Zhang, G. Hernandez, and Y. Zhu, *Opt. Lett.* **31**, 2598 (2006).
- [31] G. Huang, C. Hang, and L. Deng, *Phys. Rev. A* **77**, 011803(R) (2008).
- [32] M. Gedalin, T. C. Scott, and Y. B. Band, *Phys. Rev. Lett.* **78**, 448 (1997).
- [33] J. Yan and Y. Tang, *Phys. Rev. E* **54**, 6816 (1996); J. Yan, Y. Tang, G. Zhou, and Z. Chen, *ibid.* **58**, 1064 (1998).
- [34] Here we give only the change of the soliton parameters. In fact, a small radiation part of the soliton due to the perturbations also exists, which is omitted here.